Available online at www.sciencedirect.com
SCIENCE DIRECT
ELSEVIER
Journal of Sound and Vibration 282 (2005) 1169–1181
JOURNAL OF SOUND AND VIBRATION
www.elsevier.com/locate/jsvi

An explicit finite element method for Biot dynamic formulation in fluid-saturated porous media and its application to a rigid foundation

Chenggang Zhao[a,*], Weihua Li[a,1], Jinting Wang[b]

[a] *Department of Civil Engineering, Northern Jiao-tong University, Beijing 100044, PR China*
[b] *Post Ph.D School of Civil Engineering and Hydropower Engineering, Tsing Hua University, Beijing 100084, PR China*

Received 27 March 2003; received in revised form 8 September 2003; accepted 25 March 2004
Available online 15 December 2004

Abstract

An explicit finite element method for Biot dynamic formulation in fluid-saturated porous media is proposed. The decoupling-technique is used in the explicit finite element method. It does not need to assemble a global stiffness matrix and solve a set of linear equations in each time step, so the computational effort and memory requirement can be reduced considerably by using this method. The method is applied to analyze the dynamic response of a massless rigid foundation in a fluid-saturated porous medium. The computational results are compared with those of the elastic solution in a single-phase medium for the same problem, and it shows that if the frequency of the incident movement on rigid foundation is high (close 10 Hz), the dynamic response of the rigid foundation in fluid-saturated porous media is larger than that in single-phase media.

1. Introduction

How to solve and analyze the dynamic response of an earth structure and a site in a two-phase fluid saturated porous media is important in earthquake engineering and soil dynamics. Biot [1]

*Corresponding author.
E-mail address: lisabjjd@163.com (C. Zhao).
[1] Also for correspondence.

doi:10.1016/j.jsv.2004.03.073

developed the propagation theory of elastic waves in fluid-saturated porous media, Biot's work is a milestone that sets the foundation to solve and analyze the above-mentioned problems. Complicated equations given in Biot dynamic theory can be solved by analytical methods with some simple boundary conditions. Most dynamic problems in fluid-saturated porous media are solved using numerical methods, especially using finite element methods. Zhao et al. [2] presented a review of wave propagation theory in fluid-saturated porous media and its numerical methods. Ghaboussi and Wilson [3], Zienkiewicz et al. [4], Prevost [5], Aubry [6] and others have researched finite element methods applied to the dynamic problems in a fluid-saturated porous media. If the finite element methods are used in the time domain, there is a disadvantage in them, which require dividing time into time steps and solving a set of linear equations within each time step. These methods are suitable when problems are with a few degrees of freedom. For problems with a large number of degrees of freedom, the computational effort and memory requirement will be increased enormously, so the application of these methods to practical problems is limited. To overcome the disadvantage of these methods, an explicit finite element method for Biot dynamic formulation in a fluid-saturated porous media is proposed in this paper. Because the decoupling-technique is employed, the kinetic movement of a node is only relative to its adjacent nodes. The excellent characteristics of this method are that the global stiffness matrix does not need to be assembled and the linear equations do not need to be solved, so the computational effort and memory requirement can be reduced considerably. The method is combined with the local transmitting artificial boundary that was proposed by Liao [7], and becomes a complete and effective method to solve dynamic problems in a fluid-saturated porous media for plane strain problems (for two dimension). The calculation results are shown that for a dynamic problem (two dimension) with 3000 time steps and 1600 nodes in a fluid-saturated porous medium, only 270 s CPU time is needed on a 200 MHz 586PC. Since the method is more efficient, it may have promising future in practical applications.

2. Biot dynamic equations for saturated porous media

Biot dynamic equations for saturated porous media are

$$
\begin{aligned}
&N\nabla^2 u + \nabla[(A+N)e + Q\varepsilon] = (\rho_{11}\ddot{u} + \rho_{12}\ddot{U}) + b(\dot{u} - \dot{U}),\\
&\nabla[Qe + R\varepsilon] = (\rho_{12}\ddot{u} + \rho_{22}\ddot{U}) - b(\dot{u} - \dot{U}),
\end{aligned} \tag{1}
$$

where $\mathbf{u}$ and $\mathbf{U}$ are the displacements of solid and liquid phase, respectively, $e = \nabla\mathbf{u}$, $\varepsilon = \nabla\mathbf{U}$, $\rho_{11} = \rho_1 + \rho_a$, $\rho_{22} = \rho_2 + \rho_a$, $\rho_{12} = -\rho_a$, and $\rho_1 = (1-n)\rho_s$; $\rho_2 = n\rho_f$, ρ_s is the density of solid mass, ρ_f is the density of liquid mass, ρ_a is the density of coupled-mass between solid and liquid phase (ρ_a is difficult to be measured). The coefficient b is relative to permeability, $b = \zeta n^2/k$; ζ represents the coefficient of fluid viscosity, n represents porosity, and k represents the coefficient of permeability. N and A are similar to Lame constants μ and λ in elastic theory. R and Q are obtained by experiments. Biot [1] presented all the above parameters in detail.

3. The formulae for the explicit finite element method

To formulate the problem, it is assumed that $\rho_a = 0$ and two-dimensional plane strain elements are used [4].

3.1. Representing Biot dynamic equations in matrix form

Biot dynamic equations for saturated porous media in the matrix form can be obtained expressed as follows:

$$\begin{aligned}
&[L]^{\mathrm{T}}[D_1][L]\{u\} + [L]^{\mathrm{T}}[D_2][L]\{U\} = \rho_{11}\{\ddot{u}\} + b(\{\dot{u}\} - \{\dot{U}\}),\\
&[L]^{\mathrm{T}}[D_2][L]\{u\} + [L]^{\mathrm{T}}[D_3][L]\{U\} = \rho_{22}\{\ddot{U}\} - b(\{\dot{u}\} - \{\dot{U}\}),
\end{aligned} \tag{2}$$

where

$$[L]^{\mathrm{T}} = \begin{bmatrix} \dfrac{\partial}{\partial x} & 0 & \dfrac{\partial}{\partial y} \\ 0 & \dfrac{\partial}{\partial y} & \dfrac{\partial}{\partial x} \end{bmatrix}; \quad \{u\} = \begin{Bmatrix} u_x \\ u_y \end{Bmatrix}; \quad \{U\} = \begin{Bmatrix} U_x \\ U_y \end{Bmatrix};$$

$$[D_1] = \begin{bmatrix} A+2N & A & 0 \\ A & A+2N & 0 \\ 0 & 0 & N \end{bmatrix}; \quad [D_2] = \begin{bmatrix} Q & Q & 0 \\ Q & Q & 0 \\ 0 & 0 & 0 \end{bmatrix}; \quad [D_3] = \begin{bmatrix} R & R & 0 \\ R & R & 0 \\ 0 & 0 & 0 \end{bmatrix}.$$

3.2. Expressions of finite element equations

Finite element discretization on the considering domain is performed. Displacements and forces in the element e for two phases are represented as follows:

$$\{\mathbf{u}\}^e = [N]\{\mathbf{u}_e\}; \quad \{\mathbf{U}\}^e = [N]\{\mathbf{U}_e\}, \tag{3}$$

$$\{\mathbf{f}\}^e = [N]\{\mathbf{f}_e\}; \quad \{\mathbf{F}\}^e = [N]\{\mathbf{F}_e\}. \tag{4}$$

In Eqs. (3) and (4), $[N]$ is the shape function of the element; $\{\mathbf{u}_e\}, \{\mathbf{U}_e\}$ and $\{\mathbf{f}_e\}, \{\mathbf{F}_e\}$ represent the nodal displacements and the nodal forces of solid and liquid phases in the element e, respectively; $\{\mathbf{u}\}^e, \{\mathbf{U}\}^e$ and $\{\mathbf{f}\}^e, \{\mathbf{F}\}^e$ represent the displacements and forces of solid and liquid phases inside the element e, respectively. By making use of Galerkin method, we can get the finite element equations of node 1 in a local element system

$$\sum_{L=1}^{4}\sum_{j=1}^{4} M_{s1j}^{L}\ddot{u}_j^{L} + \sum_{L=1}^{4}\sum_{j=1}^{4} C_{1j}^{L}\left(\dot{u}_j^{L} - \dot{U}_j^{L}\right) + \sum_{L=1}^{4}\sum_{j=1}^{4} K_{ss1j}^{L}u_j^{L} + \sum_{L=1}^{4}\sum_{j=1}^{4} K_{sL1j}^{L}U_j^{L} = \sum_{L=1}^{4} f_1^{L}, \tag{5}$$

$$\sum_{L=1}^{4}\sum_{j=1}^{4} M_{L1j}^{L}\ddot{U}_j^{L} - \sum_{L=1}^{4}\sum_{j=1}^{4} C_{1j}^{L}\left(\dot{u}_j^{L} - \dot{U}_j^{L}\right) + \sum_{L=1}^{4}\sum_{j=1}^{4} K_{Ls1j}^{L}u_j^{L} + \sum_{L=1}^{4}\sum_{j=1}^{4} K_{LL1j}^{L}U_j^{L} = \sum_{L=1}^{4} F_1^{L}. \tag{6}$$

In Eqs. (5) and (6), L represents the influences of adjacent elements on node 1 and j represents the influences of four nodes in the same element on node 1. Putting every node i equal to 1, we can give any nodal equations and in this way we can get the total equations. In this method the response of every node can be calculated individually. This method is similar to finite difference methods for wave propagation, except those do not need to integrate a set of simultaneous equations.

To simplify calculation, the following decoupling method is used. It is assumed that the variance of inertia force in an element can be neglected. It is reasonable. For accuracy to simulate wave motion problem, the size of an element must be much less than the wavelength, and the variance of inertia force in the element is little. In this way the mass matrix is decoupling. According to this assumption we can get the following equations:

$$\ddot{u}_j^e = \ddot{u}_1; \quad \ddot{U}_j^e = \ddot{U}_1 \quad (j = 1, 2, 3, 4), \tag{7}$$

$$\sum_{L=1}^{4} \sum_{j=1}^{4} M_{s1j}^L \ddot{u}_j^L = \sum_{L=1}^{4} \sum_{j=1}^{4} M_{s1j}^L \ddot{u}_1 = M_{s1} \ddot{u}_1, \tag{8}$$

$$\sum_{L=1}^{4} \sum_{j=1}^{4} M_{L1j}^L \ddot{U}_j^L = \sum_{L=1}^{4} \sum_{j=1}^{4} M_{L1j}^L \ddot{U}_1 = M_{L1} \ddot{U}_1, \tag{9}$$

$$M_{s1} = \sum_{L=1}^{4} \sum_{j=1}^{4} M_{s1j}^L; \quad M_{L1} = \sum_{L=1}^{4} \sum_{j=1}^{4} M_{L1j}^L, \tag{10}$$

$$M_{sij}^L = \int \int_{\Omega^L} \rho_{11} [N_i][N_j] \, \mathrm{d}x \, \mathrm{d}y = \int_{-1}^{1} \int_{-1}^{1} \rho_{11} [N_i][N_j] |J| \, \mathrm{d}\xi \, \mathrm{d}\eta, \tag{11}$$

$$M_{Lij}^L = \int \int_{\Omega^L} \rho_{22} [N_i][N_j] \, \mathrm{d}x \, \mathrm{d}y = \int_{-1}^{1} \int_{-1}^{1} \rho_{22} [N_i][N_j] |J| \, \mathrm{d}\xi \, \mathrm{d}\eta. \tag{12}$$

Substituting Eqs. (8) and (9) into (5) and (6), we can get

$$M_{s1} \ddot{u}_1 + \sum_{L=1}^{4} \sum_{j=1}^{4} C_{1j}^L \left(\dot{u}_j^L - \dot{U}_j^L \right) + \sum_{L=1}^{4} \sum_{j=1}^{4} K_{ss1j}^L u_j^L + \sum_{L=1}^{4} \sum_{j=1}^{4} K_{sL1j}^L U_j^L = \sum_{L=1}^{4} f_1^L, \tag{13}$$

$$M_{L1} \ddot{U}_1 - \sum_{L=1}^{4} \sum_{j=1}^{4} C_{1j}^L \left(\dot{u}_j^L - \dot{U}_j^L \right) + \sum_{L=1}^{4} \sum_{j=1}^{4} K_{Ls1j}^L u_j^L + \sum_{L=1}^{4} \sum_{j=1}^{4} K_{LL1j}^L U_j^L = \sum_{L=1}^{4} F_1^L. \tag{14}$$

Putting

$$C_{ij}^L = \int \int_{\Omega^L} b [N_i][N_j] \, \mathrm{d}x \, \mathrm{d}y = \int_{-1}^{1} \int_{-1}^{1} b [N_i][N_j] |J| \, \mathrm{d}\xi \, \mathrm{d}\eta; \quad K_{LLij}^L = \int_{-1}^{1} \int_{-1}^{1} [B_i]^{\mathrm{T}} [D_3][B_j] |J| \, \mathrm{d}\xi \, \mathrm{d}\eta;$$

$$K_{sLij}^{L} = K_{Lsij}^{L} = \int_{-1}^{1}\int_{-1}^{1}[B_i]^{\mathrm{T}}[D_2][B_j]|J|\,\mathrm{d}\xi\,\mathrm{d}\eta; \quad K_{ssij}^{L} = \int_{-1}^{1}\int_{-1}^{1}[B_i]^{\mathrm{T}}[D_1][B_j]|J|\,\mathrm{d}\xi\,\mathrm{d}\eta;$$

$$f_1^L = \int_{\Gamma^L}[N_1]\tilde{T}_s\,\mathrm{d}r; \quad F_1^L = \int_{\Gamma^L}[N_1]\left\{\begin{array}{c} n\pi \\ n\pi \end{array}\right\}\mathrm{d}r; \quad \tilde{T}_s = \left\{\begin{array}{c} \tilde{T}_x \\ \tilde{T}_y \end{array}\right\}.$$

In the above equations, $\mathbf{B} = \mathbf{LN}$, $\tilde{T}_x$ and $\tilde{T}_y$ represent distributed external forces of solid phase acting along the element boundary L in the x- and y-direction, respectively; p represents boundary pore water pressure. From Eqs. (13) and (14), it can be seen that **C** and **K** matrices are only relative to adjacent element, so they are not affected by other elements. Eqs. (13) and (14) are local relative and decoupling equations.

3.3. Dynamic response expressions of internal nodes

When an infinite domain is dealt with by using finite element methods, artificial boundaries have to be introduced, so the nodes in finite element grids can be divided into artificial boundary nodes and internal nodes. In this section, the dynamic response expressions of any internal node will be given. The dynamic response expressions of artificial boundary nodes can be represented by the dynamic responses of internal nodes and input movement, which will be stated later (see artificial boundary).

When the time step is p (time$=p\Delta t, \Delta t$ represents the time step), Eqs. (13) and (14) can be represented as

$$M_{s1}\ddot{u}_1^p + \sum_{L=1}^{4}\sum_{j=1}^{4} C_{1j}^L\left(\dot{u}_j^{L,p} - \dot{U}_j^{L,p}\right) + \sum_{L=1}^{4}\sum_{j=1}^{4} K_{ss1j}^L u_j^{L,p} + \sum_{L=1}^{4}\sum_{j=1}^{4} K_{sL1j}^L U_j^{L,p} = \sum_{L=1}^{4} f_1^{L,p}, \tag{15}$$

$$M_{L1}\ddot{U}_1^p - \sum_{L=1}^{4}\sum_{j=1}^{4} C_{1j}^L\left(\dot{u}_j^{L,p} - \dot{U}_j^{L,p}\right) + \sum_{L=1}^{4}\sum_{j=1}^{4} K_{Ls1j}^L u_j^{L,p} + \sum_{L=1}^{4}\sum_{j=1}^{4} K_{LL1j}^L U_j^{L,p} = \sum_{L=1}^{4} F_1^{L,p}. \tag{16}$$

When the time step is $p+1$ (time $= (p+1)\Delta t$), Eqs. (13) and (14) can be represented as

$$\begin{aligned} M_{s1}\ddot{u}_1^{p+1} &+ \sum_{L=1}^{4}\sum_{j=1}^{4} C_{1j}^L\left(\dot{u}_j^{L,p+1} - \dot{U}_j^{L,p+1}\right) + \sum_{L=1}^{4}\sum_{j=1}^{4} K_{ss1j}^L u_j^{L,p+1} \\ &+ \sum_{L=1}^{4}\sum_{j=1}^{4} K_{sL1j}^L U_j^{L,p+1} = \sum_{L=1}^{4} f_1^{L,p+1}, \end{aligned} \tag{17}$$

$$\begin{aligned} M_{L1}\ddot{U}_1^{p+1} &- \sum_{L=1}^{4}\sum_{j=1}^{4} C_{1j}^L\left(\dot{u}_j^{L,p+1} - \dot{U}_j^{L,p+1}\right) + \sum_{L=1}^{4}\sum_{j=1}^{4} K_{Ls1j}^L u_j^{L,p+1} \\ &+ \sum_{L=1}^{4}\sum_{j=1}^{4} K_{LL1j}^L U_j^{L,p+1} = \sum_{L=1}^{4} F_1^{L,p+1}. \end{aligned} \tag{18}$$

By putting Eq. (17) + Eq. (15) and Eq. (18) + Eq. (16), we can get

$$M_{s1}\left(\ddot{u}_1^{p+1}+\ddot{u}_1^{p}\right)+\sum_{L=1}^{4}\sum_{j=1}^{4}C_{1j}^{L}\left[\left(\dot{u}_j^{L,p+1}+\dot{u}_j^{L,p}\right)-\left(\dot{U}_j^{L,p+1}+\dot{U}_j^{L,p}\right)\right]$$
$$+\sum_{L=1}^{4}\sum_{j=1}^{4}K_{ss1j}^{L}\left(u_j^{L,p+1}+u_j^{L,p}\right)+\sum_{L=1}^{4}\sum_{j=1}^{4}K_{sL1j}^{L}\left(U_j^{L,p+1}+U_j^{L,p}\right)=\sum_{L=1}^{4}\left(f_1^{L,p+1}+f_1^{L,p}\right), \tag{19}$$

$$M_{L1}\left(\ddot{U}_1^{p+1}+\ddot{U}_1^{p}\right)-\sum_{L=1}^{4}\sum_{j=1}^{4}C_{1j}^{L}\left[\left(\dot{u}_j^{L,p+1}+\dot{u}_j^{L,p}\right)-\left(\dot{U}_j^{L,p+1}+\dot{U}_j^{L,p}\right)\right]$$
$$+\sum_{L=1}^{4}\sum_{j=1}^{4}K_{Ls1j}^{L}\left(u_j^{L,p+1}+u_j^{L,p}\right)+\sum_{L=1}^{4}\sum_{j=1}^{4}K_{LL1j}^{L}\left(U_j^{L,p+1}+U_j^{L,p}\right)=\sum_{L=1}^{4}\left(F_1^{L,p+1}+F_1^{L,p}\right). \tag{20}$$

Through central difference method in time domain, we get the following equations:

$$\left\{\dot{W}_i^{p}\right\}=\frac{1}{2\Delta t}\left(\left\{W_i^{p+1}\right\}-\left\{W_i^{p-1}\right\}\right), \tag{21}$$

$$\left\{\ddot{W}_i^{p}\right\}=\frac{1}{\Delta t^2}\left(\left\{W_i^{p+1}\right\}-2\left\{W_i^{p}\right\}+\left\{W_i^{p-1}\right\}\right), \tag{22}$$

$$\left\{\ddot{W}_i^{p}\right\}=\frac{2}{\Delta t^2}\left(\left\{W_i^{p+1}\right\}-\left\{W_i^{p}\right\}\right)-\frac{2}{\Delta t}\left\{\dot{W}_i^{p}\right\}. \tag{23}$$

In Eqs. (21)–(23), $\{W_i^q\}$, $\{\dot{W}_i^q\}$ and $\{\ddot{W}_i^q\}$ represent the displacement, velocity and acceleration of the node i at the time step q, respectively. Letting $W=u$, and U, substitute Eq. (23) into Eqs. (13) and (14), and put node 1 as node i. The displacement expressions of solid and liquid phase can be given as

$$u_i^{p+1}=u_i^{p}+\Delta t\times\dot{u}_i^{p}-\frac{\Delta t^2}{2}M_{si}^{-1}\left\{\sum_{L=1}^{4}\sum_{j=1}^{4}C_{ij}^{L}\left(\dot{u}_i^{L,p}-\dot{U}_i^{L,p}\right)+\sum_{L=1}^{4}\sum_{j=1}^{4}K_{ssij}^{L}u_j^{L,p}\right.$$
$$\left.+\sum_{L=1}^{4}\sum_{j=1}^{4}K_{sLij}^{L}U_j^{L,p}-\sum_{L=1}^{4}f_1^{L,p}\right\}, \tag{24}$$

$$U_i^{p+1}=U_i^{p}+\Delta t\times\dot{U}_i^{p}-\frac{\Delta t^2}{2}M_{Li}^{-1}\left\{-\sum_{L=1}^{4}\sum_{j=1}^{4}C_{ij}^{L}\left(\dot{u}_i^{L,p}-\dot{U}_i^{L,p}\right)+\sum_{L=1}^{4}\sum_{j=1}^{4}K_{sLij}^{L}u_j^{L,p}\right.$$
$$\left.+\sum_{L=1}^{4}\sum_{j=1}^{4}K_{LLij}^{L}U_j^{L,p}-\sum_{L=1}^{4}F_i^{L,p}\right\}. \tag{25}$$

The assumption for Newmark constant average acceleration method is given as

$$\frac{\left\{\ddot{W}_i^{p+1}\right\}+\left\{\ddot{W}_i^{p}\right\}}{2}=\frac{\left\{\dot{W}_i^{p+1}\right\}-\left\{\dot{W}_i^{p}\right\}}{\Delta t}, \tag{26}$$

$$\left\{W_i^{p+1}\right\}=\left\{W_i^{p}\right\}+\Delta t\left\{\dot{W}_i^{p}\right\}+\frac{1}{4}\Delta t^2\left(\left\{\ddot{W}_i^{p+1}\right\}+\left\{\ddot{W}_i^{p}\right\}\right). \tag{27}$$

From Eqs. (26) and (27), the following expression is deduced

$$\frac{\left\{\dot{W}_i^{p+1}\right\}+\left\{\dot{W}_i^{p}\right\}}{2}=\frac{\left\{W_i^{p+1}\right\}-\left\{W_i^{p}\right\}}{\Delta t}, \tag{28}$$

Substituting Eqs. (26) and (28) into Eqs. (19) and (20), and putting node 1 as node i. The velocity expressions of solid and liquid phase can be deduced as

$$\begin{aligned}\dot{u}_i^{p+1}=\dot{u}_i^{p}-M_{si}^{-1}\Bigg\{&\sum_{L=1}^{4}\sum_{j=1}^{4}C_{ij}^{L}\left[\left(u_j^{L,p+1}-u_j^{L,p}\right)-\left(U_j^{L,p+1}-U_j^{L,p}\right)\right]\\&+\frac{\Delta t}{2}\Bigg[\sum_{L=1}^{4}\sum_{j=1}^{4}K_{ssij}^{L}\left(u_j^{L,p+1}+u_j^{L,p}\right)\\&+\sum_{L=1}^{4}\sum_{j=1}^{4}K_{sLij}^{L}\left(U_j^{L,p+1}+U_j^{L,p}\right)-\sum_{L=1}^{4}\left(f_i^{L,P+1}+f_i^{L,p}\right)\Bigg]\Bigg\}\end{aligned} \tag{29}$$

$$\begin{aligned}\dot{U}_i^{p+1}=\dot{U}_i^{p}-M_{Li}^{-1}\Bigg\{&\sum_{L=1}^{4}\sum_{j=1}^{4}C_{ij}^{L}\left[-\left(u_j^{L,p+1}-u_j^{L,p}\right)-\left(U_j^{L,p+1}-U_j^{L,p}\right)\right]\\&+\frac{\Delta t}{2}\Bigg[\sum_{L=1}^{4}\sum_{j=1}^{4}K_{sLij}^{L}\left(u_j^{L,p+1}+u_j^{L,p}\right)\\&+\sum_{L=1}^{4}\sum_{j=1}^{4}K_{LLij}^{L}\left(U_j^{L,p+1}+U_j^{L,p}\right)-\sum_{L=1}^{4}\left(F_i^{L,p+1}+F_i^{L,p}\right)\Bigg]\Bigg\}\end{aligned} \tag{30}$$

From Eq. (26) the acceleration expressions of solid and liquid phase can be deduced as

$$\ddot{u}_i^{p+1}=-\ddot{u}_i^{p}+2\left(\dot{u}_i^{p+1}-\dot{u}_i^{p}\right)/\Delta t \tag{31}$$

$$\ddot{U}_i^{p+1}=-\ddot{U}_i^{p}+2\left(\dot{U}_i^{p+1}-\dot{U}_i^{p}\right)/\Delta t. \tag{32}$$

Eqs. (24), (25) and (29)–(32) consist of an explicit finite element solution to Eq. (1) of Biot dynamic equations in a fluid-saturated porous media. This solution's form is like an explicit finite difference form.

First, u_i^{p+1} and U_i^{p+1} (displacements in the time step $p+1$) in Eqs. (24) and (25) can be calculated by making use of the kinetic movement quantities in the time step p. Then $\dot{u}_i^{p+1}$ and $\dot{U}_i^{p+1}$ (velocities in the time step $p+1$) in Eqs. (29) and (30) can be calculated by making use of u_i^{p+1} and U_i^{p+1} and other kinetic movement quantities in the time step p. At last $\ddot{u}_i^{p+1}$ and $\ddot{U}_i^{p+1}$ (accelerations in the step time $p+1$) in Eqs. (31) and (32) can be calculated by making use of u_i^p, U_i^p and $\ddot{u}_i^p$, $\ddot{U}_i^p$, u_i^{p+1}, U_i^{p+1}. So by making use of Eqs. (24), (25), (29)–(32), we can get dynamic responses in the time step $p+1$ from the last dynamic responses in the time step p.

4. Artificial boundary

There are three types of wave (P_I, P_{II} and S waves) in a fluid-saturated porous media according to Biot dynamic theory [1]. Each type of wave propagates at an inherent velocity, i.e. for a specific type of wave no matter it is solid or liquid phase, both of them propagate at the same velocity to the same direction, but there is a fixed relationship between them. Based on the transmitting artificial boundary theory [7], we postulate that the propagation of both solid and liquid phase passes through artificial boundaries at the same velocity to the same direction. So we use transmitting artificial boundary formulae to both solid and liquid phase separately, and in this way the scattering wave fields of both solid and liquid phase along artificial boundary nodes can be calculated. Transmitting artificial boundary is a decoupling artificial boundary, it is combined with the above-mentioned decoupling explicit finite element to form a whole decouple method.

5. Comparing the explicit finite element results with analytical solution

To test the correctness and accuracy of the explicit finite element, an example is given to compare this method and an analytical solution [8], and then the results of the two methods are compared. The analytical method [8] is a one-dimensional method. But we will solve this problem in two dimensions using the method developed in this paper. First, artificial boundaries are introduced and finite element grids are discretized. The numerical model is shown in Fig. 1 (Fig. 1 is just a sketch map, not an exact map). The basic material properties are shown in Table 1.

The results, both the analytical method and the explicit finite element method developed in this paper, are shown in Figs. 2 and 3. In Fig. 2, $\xi = x/(\rho k V_c)$ is the horizontal coordinate; $\mathbf{u}$ and $\mathbf{U}$ (the displacement factors) are vertical coordinates; $\tau = t/(\rho k)$ is a time factor. Putting $\sigma_0 = 1$, the results of numerical solutions and analytical solutions at $\tau = 50, 100, 150$ are shown in Fig. 2. The displacement factors of both solid and liquid phase on free surface are shown in Fig. 3. The figures show that the numerical solutions are perfectly close to the analytical solutions, so the method developed in this paper has a very high degree of calculating accuracy.

6. Dynamic response of a rigid foundation

In seismic site response analysis or seismic soil–structure interaction analysis, it is the most common assumption that the soil is an elastic single-phase solid media. But when the soil deposit

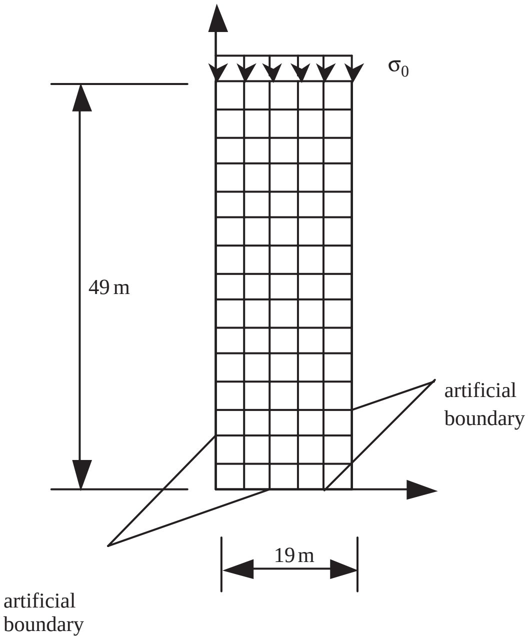

Fig. 1. The finite element model.

Table 1
Basic material properties

A (Pa)	N (Pa)	n	ρ_s (kg/m^3)	ρ_f (kg/m^3)	ρ (kg/m^3)	Q (Pa)	R (Pa)	K (cm/s)
2.38×10^7	1.25×10^7	0.333	3101	2977	3060	1.54×10^9	1.54×10^9	0.00488

is saturated cohesionless soil, it is more practical to suppose the soil to be fluid-saturated porous media, and to use Biot dynamic theory to deal with it. This theory is more advanced and can represent solid–fluid interaction, so it can simulate practical situation more accurately.

The dynamic response analyses of a rigid foundation (no mass is supposed) on the top surface of saturated cohesionless soil deposit are made by using the method developed in the paper and the elastic single-phase finite element method [9]. The purpose is to compare what differences are in dynamic results of those two methods. The model is a rigid foundation (its width is 40 m, its length is infinite and no mass in it) on the surface of a two-dimensional saturated cohesionless half infinite soil space, Fig. 4 gives a sketch map of discredited grids (not an exact one) for both methods. All finite elements are same and square; the length of an element edge in both x- and y-direction is 5 m. The material properties of two media are shown in Tables 2 and 3. In Tables 2 and 3, we want to make the material properties of the elastic single-phase media closely similar to those of the fluid-saturated porous media. There is an even-distributed sine load P acting on the rigid foundation, $P = \sigma_0 \sin(\omega t)$, where $\sigma_0 = -50\,\mathrm{KN/m^2}$.

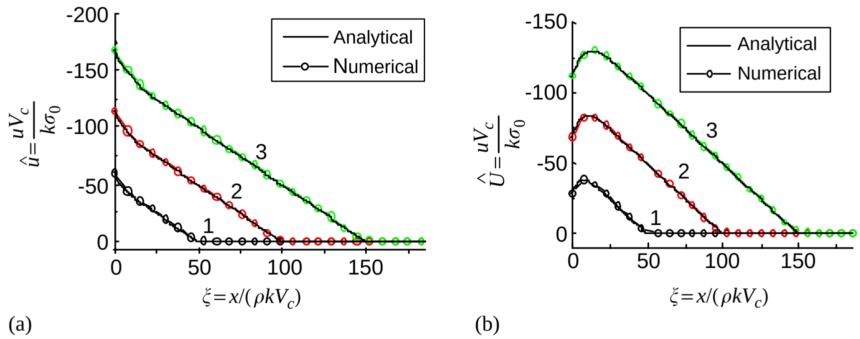

Fig. 2. Dynamic response at different time (1— =50, 2— =100, 3— =150). (a) Solid Phase, (b) fluid phase.

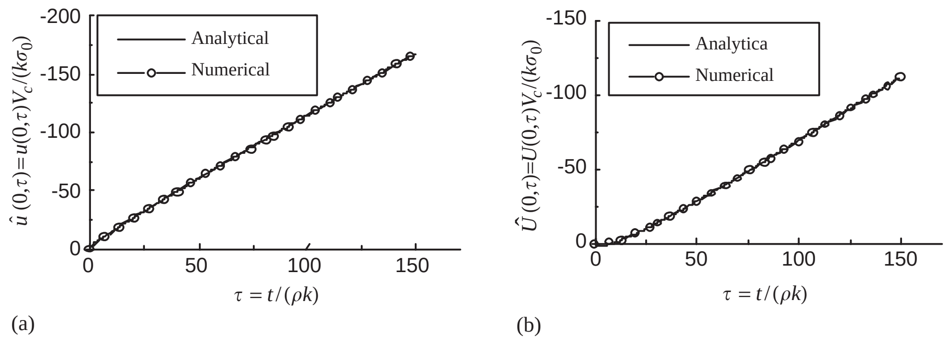

Fig. 3. The displacement on free surface. (a) Solid phase, (b) fluid phase.

Using explicit finite element method developed in this paper to analyze the dynamic response of the rigid foundation, the following assumptions should be satisfied to simplify the calculation: $u_y = u_{ys} = U_{yL}$; $u_x = u_{xs} = 0$.

Using the elastic single-phase finite element method [9] to analyze dynamic response of a rigid foundation, the following assumptions should be satisfied to simplify the calculation:

(1) The vertical displacements on the interface between rigid foundation and the elastic half infinite space are same.
(2) The horizontal displacements on the interface are supposed to be *zero*.

The displacement in an elastic single-phase media at the middle point of the interface between the rigid foundation and soil, and the displacement of solid phase in saturated porous media at the middle point of interface, are shown in Fig. 5. The load frequencies are $f = 0.2, 1, 2$, and 10 Hz, respectively. In Fig. 5, the horizontal coordinate is time, and vertical coordinate is the vertical displacement at the middle point of the interface.

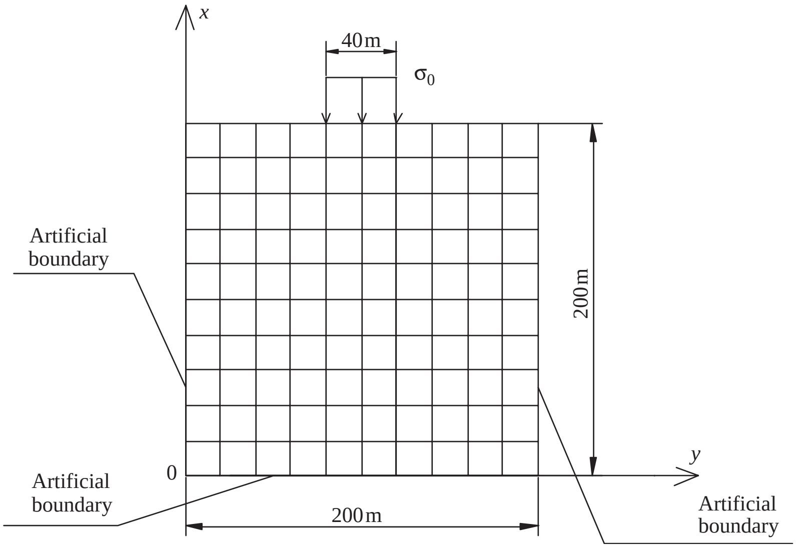

Fig. 4. Element meshing of two models.

Table 2
Material properties of elastic single-phase media

ρ (kg/m^3)	λ (Pa)	μ (Pa)
3060	8.33×10^7	1.25×10^7

Table 3
Material properties of fluid-saturated porous media

A (Pa)	N (Pa)	n	ρ_s (kg/m^3)	ρ_f (kg/m^3)	ρ (kg/m^3)	Q (Pa)	R (Pa)	K (cm/s)
2.38×10^7	1.25×10^7	0.333	3101	2977	3060	1.54×10^9	1.54×10^9	0.00488

Fig. 5 shows that there are some different dynamic responses at the foregoing conditions. While incident load frequency is high (such as $f = 10\,\text{Hz}$), the solid phase dynamic displacement in the saturated porous media is larger than that in an elastic single-phase media. On the contrary, while incident load frequency is low (such as $f = 0.2\,\text{Hz}$), the solid phase dynamic displacement in saturated porous media is smaller than that in an elastic single-phase media. The analysis shows that, in the above-mentioned conditions, it is better to use the Biot dynamic theory method developed in the paper to analyze dynamic response of saturated cohesionless soil for high-frequency loading.

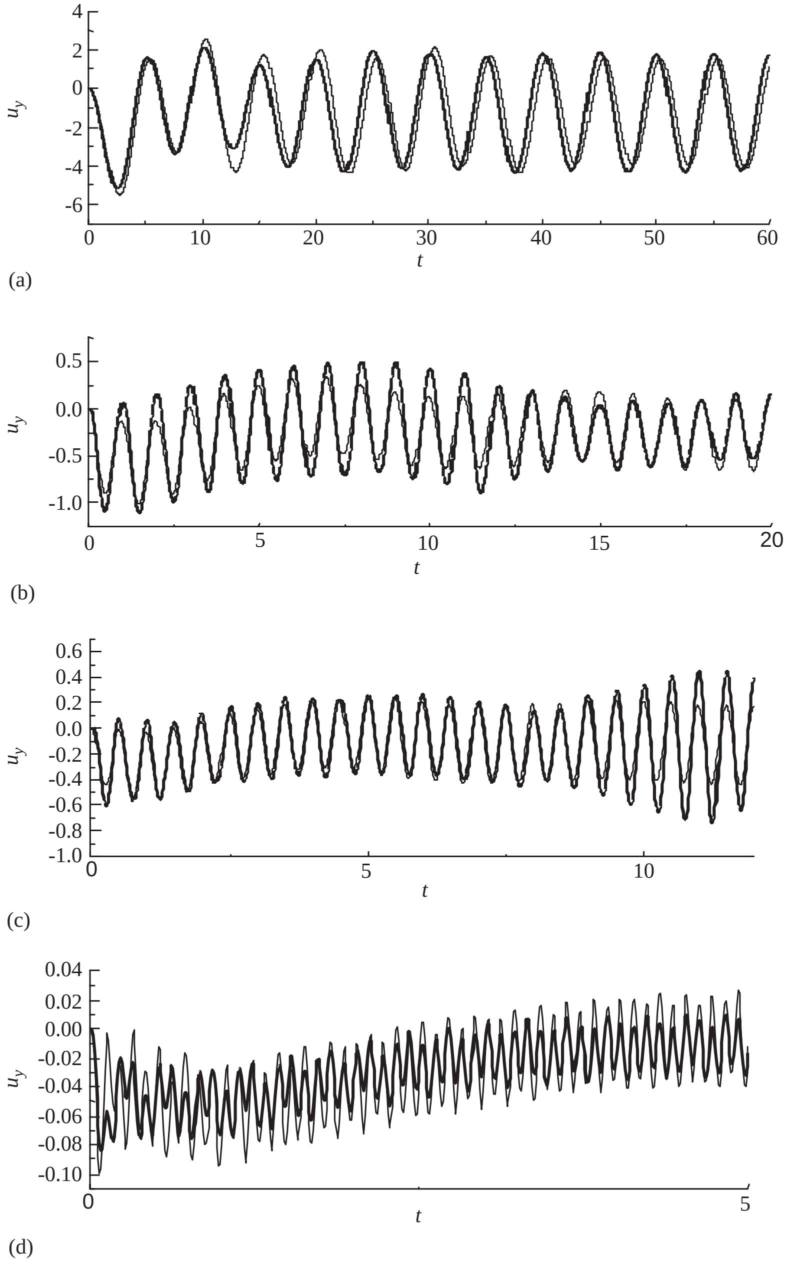

Fig. 5. The vertical displacement of midpoint at rigid foundation (the thin curve indicates the solutions of two-phase media; the thick curve indicates the solutions of elastic single-phase media). (a) $f = 0.2\,\text{Hz}$, (b) $f = 1\,\text{Hz}$, (c) $f = 2\,\text{Hz}$, (d) $f = 10\,\text{Hz}$.

The calculation results using the proposed method have shown that for this dynamic problem (two dimension) with 3000 time steps and 1600 nodes in a fluid-saturated porous medium, only 270 s CPU time is needed on a 200 MHz 586PC.

7. Closing remark

In the paper, an explicit finite element method for dynamic response analysis with fluid-saturated porous media has been developed. The comparing dynamic response analyses of a rigid foundation between the fluid-saturated porous media and elastic single-phase media are given. The results show that while incident load frequency is high (close 10 Hz), to analyze dynamic response of saturated cohesionless soil, using the fluid-saturated porous media model is more practical. It also shows that computational effort and memory requirement can be reduced considerably by using the method developed in the paper.

Acknowledgements

The reported work was supported by the Natural Science Foundation of P. R. C. (Grant No. 50178005).

References

[1] M.A. Biot, Theory of elastic wave in fluid-saturated porous solid, *The Journal of the Acoustical Society of America* 28 (1956) 168–178.
[2] C.G. Zhao, et al., Review of wave propagation theory in saturated and unsaturated porous media and its numerical methods, *Advances in Mechanics* 28 (1998) 83–92 (in Chinese).
[3] J. Ghaboussi, E.L. Wilson, Variational formulation of dynamics of fluid saturated porous elastic solids, *Journal of Engineering Mechanics Division, ASCE* 98 (1972) 947–963.
[4] O.C. Zienkiewicz, et al., Dynamic behavior of saturated porous media: the generalized Biot formulation and its numerical solution, *International Journal of Numerical and Analytical Method in Geomechanics* 8 (1984) 71–96.
[5] J.H. Prevost, Wave propagation in fluid-saturated porous media: an efficient finite element procedure, *Soil Dynamics and Earthquake Engineering* 4 (1985) 183–201.
[6] D. Aubry, Computational soil dynamics and soil–structure interaction, in: P. Gülkan, R.W. Clough (Eds.), *Development in Dynamic Soil–Structure Interaction*, 1993, pp. 43–60.
[7] Z.P. Liao, H.L. Wong, A transmitting boundary for the numerical simulation of wave propagation, *Soil Dynamics and Earthquake Engineering* 3 (1984) 176–183.
[8] B.R. Simon, et al., An analytical solution for the transient response of saturated porous elastic solids, *International Journal of Numerical and Analytical Method in Geomechanics* 8 (1984) 381–398.
[9] J.B. Liu, Z.P. Liao, A numerical method for problems of seismic wave scattering, *Earthquake Engineering and Engineering Vibration* 7 (1987) 1–18 (in Chinese).